AMERICAN SOCIETY FOR MICROBIOLOGY | Journal of Virology

Varicella-Zoster Virus Downregulates Programmed Death Ligand 1 and Major Histocompatibility Complex Class I in Human Brain Vascular Adventitial Fibroblasts, Perineurial Cells, and Lung Fibroblasts

Dallas Jones,[a] Anna Blackmon,[a] C. Preston Neff,[b] Brent E. Palmer,[b] Don Gilden,[a,c] Hussain Badani,[a] Maria A. Nagel[a]

Department of Neurology, University of Colorado School of Medicine, Aurora, Colorado, USA[a]; Department of Medicine, Division of Allergy and Clinical Immunology, University of Colorado School of Medicine, Aurora, Colorado, USA[b]; Department of Immunology and Microbiology, University of Colorado School of Medicine, Aurora, Colorado, USA[c]

ABSTRACT

Varicella-zoster virus (VZV) vasculopathy produces stroke, giant cell arteritis, and granulomatous aortitis, and it develops after virus reactivates from ganglia and spreads transaxonally to arterial adventitia, resulting in persistent inflammation and pathological vascular remodeling. The mechanism(s) by which inflammatory cells persist in VZV-infected arteries is unknown; however, virus-induced dysregulation of programmed death ligand 1 (PD-L1) may play a role. Specifically, PD-L1 can be expressed on virtually all nucleated cells and suppresses the immune system by interacting with the programmed cell death protein receptor 1, found exclusively on immune cells; thus, downregulation of PD-L1 may promote inflammation, as seen in some autoimmune diseases. Both flow cytometry and immunofluorescence analyses to test whether VZV infection of adventitial cells downregulates PD-L1 showed decreased PD-L1 expression in VZV-infected compared to mock-infected human brain vascular adventitial fibroblasts (HBVAFs), perineural cells (HPNCs), and fetal lung fibroblasts (HFLs) at 72 h postinfection. Quantitative RT-PCR analyses showed no change in PD-L1 transcript levels between mock- and VZV-infected cells, indicating a posttranscriptional mechanism for VZV-mediated downregulation of PD-L1. Flow cytometry analyses showed decreased major histocompatibility complex class I (MHC-I) expression in VZV-infected cells and adjacent uninfected cells compared to mock-infected cells. These data suggest that reduced PD-L1 expression in VZV-infected adventitial cells contribute to persistent vascular inflammation observed in virus-infected arteries from patients with VZV vasculopathy, while downregulation of MHC-I prevents viral clearance.

IMPORTANCE

Here, we provide the first demonstration that VZV downregulates PD-L1 expression in infected HBVAFs, HPNCs, and HFLs, which, together with the noted VZV-mediated downregulation of MHC-I, might foster persistent inflammation in vessels, leading to pathological vascular remodeling during VZV vasculopathy and persistent inflammation in infected lungs to promote subsequent infection of T cells and hematogenous virus spread. Identification of a potential mechanism by which persistent inflammation in the absence of effective viral clearance occurs in VZV vasculopathy and VZV infection of the lung is a step toward targeted therapy of VZV-induced disease.

Varicella-zoster virus (VZV) is a common, neurotropic DNA alphaherpesvirus that causes varicella (chickenpox) upon primary infection, after which virus becomes latent in ganglionic neurons along the entire neuraxis (1–6). With a decline in VZV-specific cell-mediated immunity, VZV reactivates in elderly or immunocompromised individuals, most commonly causing zoster (shingles). VZV can also reactivate and spread transaxonally to cerebral arteries to produce stroke with or without rash (VZV vasculopathy). Recent studies show that aside from stroke, VZV vasculopathy presents as giant cell arteritis, which is the most common cause of systemic vasculitis in the elderly (7), as well as granulomatous aortitis (8).

Studies of VZV-infected cerebral and temporal arteries from patients with VZV vasculopathy show viral antigen predominantly in the outermost adventitia in early infection, supporting deposition of virus from nerve fibers that terminate within this layer followed by transmural spread (7, 9). Persistent inflammation with a predominance of T cells and macrophages can be seen even up to 10 months after disease onset and is associated with pathological vascular remodeling (10). The mechanism(s) by which inflammatory cells persist to cause vascular damage in VZV-infected arteries is unknown.

Programmed cell death ligand 1 (PD-L1), a 40-kDa type 1 transmembrane protein in the B7 immunoglobulin family that can be expressed on virtually all nucleated cells (11), suppresses the immune system through interaction with its receptor, pro-

Received 3 August 2016 **Accepted** 8 September 2016

Accepted manuscript posted online 14 September 2016

Citation Jones D, Blackmon A, Neff CP, Palmer BE, Gilden D, Badani H, Nagel MA. 2016. Varicella-zoster virus downregulates programmed death ligand 1 and major histocompatibility complex class i in human brain vascular adventitial fibroblasts, perineurial cells, and lung fibroblasts. J Virol 90:10527–10534. doi:10.1128/JVI.01546-16.

Editor: R. M. Sandri-Goldin, University of California, Irvine

Address correspondence to Maria A. Nagel, maria.nagel@ucdenver.edu.

grammed cell death protein 1 (PD-1), which is expressed on activated T cells, B cells, and macrophages. The interaction between PD-L1 and PD-1 leads to the exhaustion of immune cells and promotion of apoptosis in these cells. In cancer, induction of PD-L1 is a common occurrence that can prevent immune clearance of malignant cells. Similarly, viruses such as human immunodeficiency virus (HIV) can induce PD-L1 in immune cells to avoid immune clearance (12). In contrast, several autoimmune diseases, such as systemic lupus erythematosus (SLE) and rheumatoid arthritis (RA), frequently lead to downregulation of PD-L1 and PD-1 expression, producing persistent inflammation (13).

To test whether downregulation of PD-L1 on target cells plays a role in VZV vasculopathies, we examined VZV-induced alterations of this protein in (i) primary human brain vascular adventitial fibroblasts (HBVAFs), which are among the initial cells infected following virus deposition in the artery and are key regulators of vascular tone and function, (ii) primary human perineural cells (HPNCs), which surround the nerve fiber and form a barrier between the nerve and adventitial fibroblasts, and (iii) human fetal lung fibroblasts (HFLs), which are infected during respiratory spread of VZV upon primary infection.

MATERIALS AND METHODS

Cell culture. HBVAFs (Sciencell, Carlsbad, CA), HPNCs (Sciencell), and HFLs (ATCC, Manassas, VA) were seeded at a density of 2,000 cells/cm^2 in basal fibroblast medium supplemented with 2% fetal bovine serum (FBS), 1% fibroblast growth serum, and 1% 100× penicillin-streptomycin (Sciencell). After 24 h, the medium was changed to basal fibroblast medium supplemented with 0.1% FBS and 1% 100× penicillin-streptomycin that was replenished every 48 to 72 h for 6 to 7 days to establish quiescence. At day 7, quiescent HBVAFs, HPNCs, and HFLs were cocultivated with the respective VZV-infected (25 to 30 PFU/ml) or uninfected (mock-infected) cells; as a positive control for major histocompatibility complex class I (MHC-I) and PD-L1 induction, uninfected quiescent HBVAFs and HFLs were also treated with tumor necrosis factor alpha (TNF-α; 100 ng/ml; Millipore, Billerica, MA) for 24 h, and HPNCs were treated with gamma interferon (IFN-γ; 100 ng/ml; Cell Signaling, Danvers, MA) for 24 h. Cells were harvested using sodium citrate (14) to optimize detection of cell surface proteins by flow cytometry analysis at 24 h postinfection (hpi) for TNF-α- and IFN-γ-treated cells and at 24 and 72 hpi for mock- and VZV-infected cells.

Flow cytometry (FACS). Mock- and VZV-infected cells at 24 and 72 hpi were washed with fluorescence-activated cell sorting (FACS) buffer (phosphate-buffered saline containing 1% FBS) and stained with mouse anti-human PD-L1 antibody (APC; eBioscience, San Diego, CA), mouse anti-human MHC-I antibody (phycoerythrin-Cy7; eBioscience), and mouse anti-VZV-gE (Millipore) antibody conjugated to R-phycoerythrin using the SiteClick antibody labeling kit (ThermoFisher, Waltham, MA) for 30 min at 4°C, washed with FACS buffer, and fixed with 1% paraformaldehyde. Fluorescence-minus-one (FMO) and isotype controls were used in all stainings. Cells were analyzed using a Canto-II or LSR-II flow cytometer (BD Immunocytometry Systems, San Jose, CA); >15,000 events were collected for all samples. Electronic compensation was performed with antibody capture beads (BD Biosciences, San Jose, CA), with subsequent data analyzed using Diva software (BD Biosciences) and FlowJo software (Tree Star, Ashland, OR).

Quantitative PCR analysis. Total RNA was extracted using TRIzol reagent (Thermo Fisher, Waltham, MA) at 72 hpi from mock- and VZV-infected cells; RNA was extracted from IFN-γ/TNF-α-treated cells after 24 h of treatment. Residual DNA was enzyme degraded using the Turbo DNA-free kit (Thermo-Fisher, Grand Island, NY). First-strand cDNA synthesis was carried out using the Transcriptor first-strand cDNA synthesis kit (Roche, San Francisco, CA). Primers specific for PD-L1 (15) and RPL13a (16) were used for amplification, and results were analyzed using the $\Delta\Delta C_T$ method. Gene expression is represented as fold change in virus-infected versus mock-infected cells or cytokine-treated versus mock-infected cells.

Immunofluorescence. HFLs, HBVAFs, and HPNCs were propagated on coverslips, grown to quiescence, mock infected, VZV infected, or treated with cytokines as described above and fixed using 4% paraformaldehyde. Cells were stained with mouse anti-human VZV-gE (Santa Cruz Biotechnology, Santa Cruz, CA) and rabbit anti-human PD-L1 (Abcam, Cambridge, MA). Secondary antibodies consisted of Alexa Fluor 594 donkey anti-mouse IgG or Alexa Fluor 488 donkey anti-rabbit IgG (Life-Technologies, Grand Island, NY). Coverslips were mounted with Vectashield containing 4′,6-diamidino-2-phenylindole (DAPI; Vector Laboratories, Burlingame, CA) and visualized by fluorescence microscopy.

Statistical analysis. Statistical analysis was performed using GraphPad Prism (GraphPad, San Diego, CA). Statistical significance was determined using the Student's paired *t* test.

RESULTS

VZV-mediated downregulation of PD-L1 and MHC-I expression in primary HFLs, HBVAFs, and HPNCs. In 6 independent experiments, PD-L1 mean fluorescence intensity (MFI) at 24 hpi did not differ significantly among VZV-infected HFLs, uninfected bystander HFLs, and mock-infected HFLs (923, 870, and 907, respectively) (Fig. 1A and B) or among VZV-infected HBVAFs, uninfected bystander HBVAFs, and mock-infected HBVAFs (591, 564, and 555, respectively) (Fig. 2A and B), but it was significantly increased in VZV-infected HPNCs compared to mock-infected HPNCs (1,187 and 926, respectively; $P = 0.04$) (Fig. 3A and B). At 72 hpi, PD-L1 MFI in VZV-infected HFLs was significantly decreased (665) compared to uninfected bystander (792; $P = 0.03$) or mock-infected cells (835; $P = 0.02$). Similarly, the PD-L1 MFI was significantly decreased in VZV-infected HBVAFs (296) compared to uninfected bystander (545; $P = 0.009$) or mock-infected cells (532; $P = 0.009$), as well as in VZV-infected HPNCs (619) compared to uninfected bystander (942; $P = 0.004$) or mock-infected cells (913; $P = 0.002$).

At 24 hpi, PD-L1 MFI in positive-control TNF-α-treated HFLs, positive-control TNF-α-treated HBVAFs, and positive-control IFN-γ-treated HPNCs was significantly increased (2,165 [$P < 0.01$], 1,268 [$P < 0.001$], and 2,968 [$P < 0.001$], respectively) compared to all cells analyzed at both 24 and 72 hpi. Flow cytometry analyses of PD-L1 expression at 72 hpi in mock-infected (blue) or VZV$^+$ (red) cells as well as cytokine-treated cells (orange) was displayed using histograms to show total PD-L1 downregulation (Fig. 1C, 2C, and 3C).

In the experiments described above, there was no significant change in MHC-I MFI at 24 hpi among VZV-infected HFLs, uninfected bystander HFLs, and mock-infected HFLs (5,575, 5,344, and 5,707, respectively) (Fig. 1D and E) or among VZV-infected HPNCs, uninfected bystander HPNCs, and mock-infected HPNCs (7,772, 8,291, and 8,450, respectively) (Fig. 3D and E), whereas the MHC-I MFI was significantly decreased in both VZV-infected HBVAFs (5,532) and uninfected bystander HBVAFs (5,166) compared to mock-infected HBVAFs (7,492; $P = 0.04$ and 0.02, respectively) (Fig. 2D and E). At 72 hpi, MHC-I MFI was significantly reduced in both VZV-infected HFLs (4,139) and uninfected bystander cells (4,461) compared to mock-infected cells (7,256; $P = 0.0001$ and 0.0007, respectively) and in both VZV-infected HBVAFs (3,553) and uninfected HBVAFs (5,068) com-

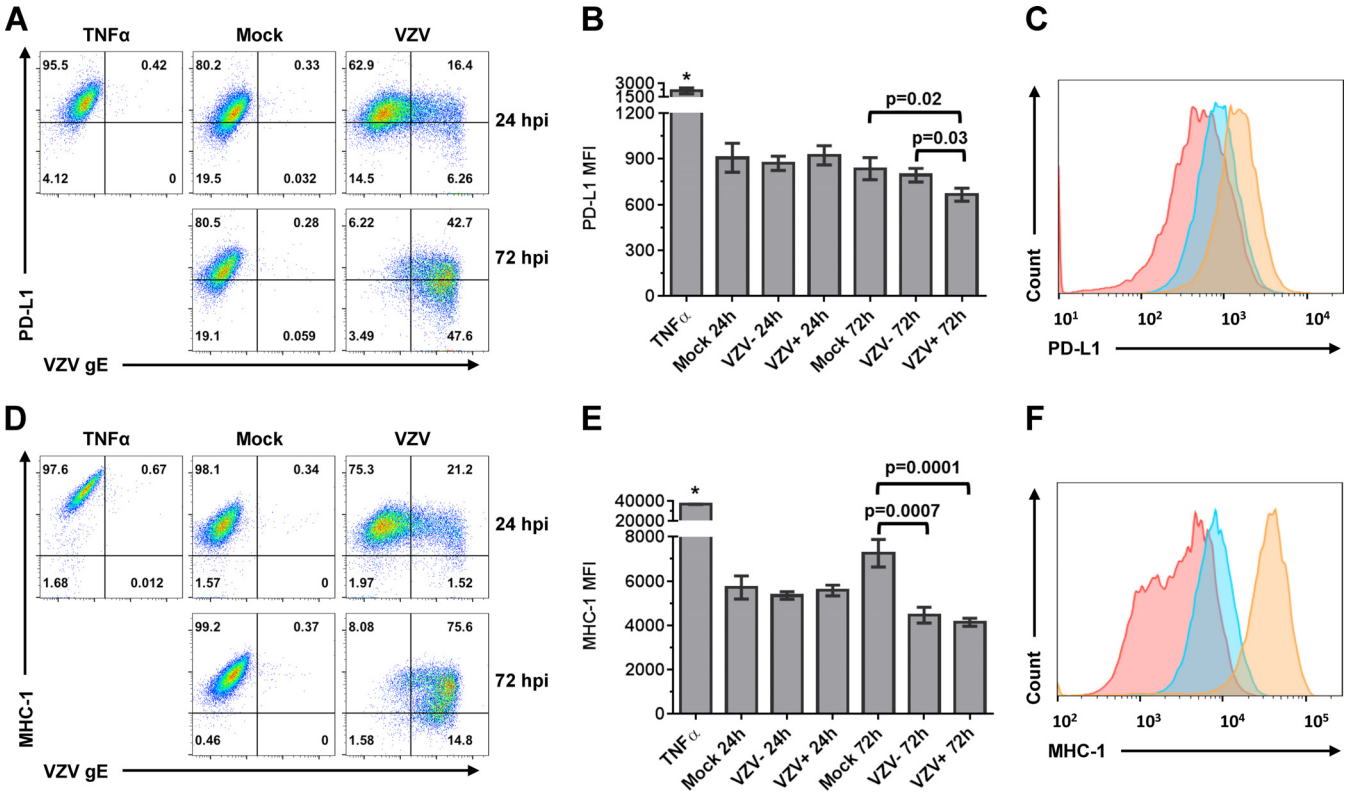

FIG 1 VZV-mediated downregulation of PD-L1 and MHC-I expression in primary human fetal lung fibroblasts (HFLs). Mock- or VZV-infected HFLs at 24 and 72 hpi, as well as positive-control TNF-α-treated HFLs at 24 h posttreatment, were harvested and analyzed by three-color flow cytometry using anti-VZV gE and anti-PD-L1 antibodies (A to C) or anti-VZV gE and anti-MHC-I antibodies (D to F); cells were gated using isotype and fluorescence-minus-one (FMO) controls. Flow cytometry plots (A) and corresponding bar graphs (B) after immunostaining with VZV gE and PD-L1 antibodies showed a significant reduction in PD-L1 MFI in VZV-infected (VZV+ 72 h) HFLs at 72 hpi compared to adjacent uninfected cells (VZV− 72 h; $P = 0.03$) or to mock-infected cells (mock 72 h; $P = 0.02$). (C) Histogram flow cytometry analyses at 72 hpi show total downregulation of PD-L1 MFI expression in VZV$^+$ (red) cells compared to mock-infected (blue) or TNF-α-treated (orange) cells. Flow cytometry plots (D) and corresponding bar graphs (E) after immunostaining with VZV gE and MHC-I antibodies showed a significant reduction in MHC-I MFI in VZV-infected HFLs at 72 hpi (VZV+ 72 h; $P = 0.0001$) and adjacent uninfected cells (VZV− 72 h) ($P = 0.0007$) compared to mock-infected cells. (F) Histogram flow cytometry analyses at 72 hpi show total downregulation of MHC-I MFI expression in VZV$^+$ (red) cells compared to mock-infected (blue) or TNF-α-treated (orange) cells. All results shown are representative of 6 independent experiments, with bar graphs representing average MFI values and error bars representing standard deviations. Statistical significance was determined using the Student *t* test. *, $P < 0.01$ for HFLs treated with TNF-α for 24 h compared to mock- and VZV-infected HFLs analyzed at 24 and 72 hpi.

pared to mock-infected HBVAFs (7,492; $P = 0.003$ and 0.008, respectively), as well as in both VZV-infected HPNCs (4,459) and uninfected bystander cells (7,028) compared to mock-infected cells (8,774; $P = 0.002$ and 0.03, respectively). In addition, the MHC-I MFI was significantly lower in both VZV-infected HBVAFs and VZV-infected HPNCs compared to their respective uninfected bystander cells ($P = 0.02$ and $P = 0.008$, respectively).

At 24 hpi, MHC-I MFI was significantly increased in positive-control HFLs, positive-control TNF-α-treated HBVAs, and positive-control IFN-γ-treated HPNCs (36,659 [$P < 0.01$], 24,303, [$P < 0.001$], and 39,039, [$P < 0.001$], respectively) compared to all cells analyzed at both 24 and 72 hpi. Flow cytometry analyses of MHC-I expression at 72 hpi in mock-infected (blue) or VZV$^+$ (red) cells as well as cytokine-treated cells (orange) was displayed using histograms to show total MHC-I downregulation (Fig. 1F, 2F, and 3F).

VZV-mediated regulation of *PD-L1* gene expression in HFLs, HBVAFs, and HPNCs. Compared to mock-infected cells, *PD-L1* gene expression in VZV-infected HFLs decreased 0.84- ± 0.28-fold, while the control TNF-α-treated HFLs showed a 5.96- ± 0.98-fold increase in such expression ($P < 0.01$) (Fig. 4A). VZV-infected HBVAFs and TNF-α-treated HBVAFs showed a 1.06- ± 0.21-fold and a 7.56- ± 4.12-fold increase, respectively, in *PD-L1* gene expression compared to mock-infected cells ($P < 0.01$) (Fig. 4B). In VZV-infected HPNCs, *PD-L1* gene expression was decreased 0.87- ± 0.63-fold but was increased 40.59- ± 11.64-fold in IFN-γ-treated HPNCs compared to mock-infected cells ($P < 0.01$) (Fig. 4C). These results indicate that the VZV-mediated inhibition of PD-L1 expression occurs at the posttranscriptional level.

Immunofluorescence analysis of PD-L1 and VZV gE expression in mock- and VZV-infected HFLs, HBVAFs, and HPNCs. At 72 hpi, mock- and VZV-infected HFLs, HBVAFs, and HPNCs were analyzed by dual immunofluorescence using a rabbit anti-PD-L1 antibody and a mouse anti-VZV gE antibody. Mock-infected HFLs, HBVAFs, and HPNCs expressed PD-L1 (green) but not VZV gE (red) (Fig. 5A, rows 1, 3, and 5, respectively), whereas VZV-infected HFLs, HBVAFs, and HPNCs expressed VZV gE with minimal/no expression of PD-L1 (Fig. 5A, rows 2, 4, and 6, respectively). Positive controls for PD-L1 expression (green) were

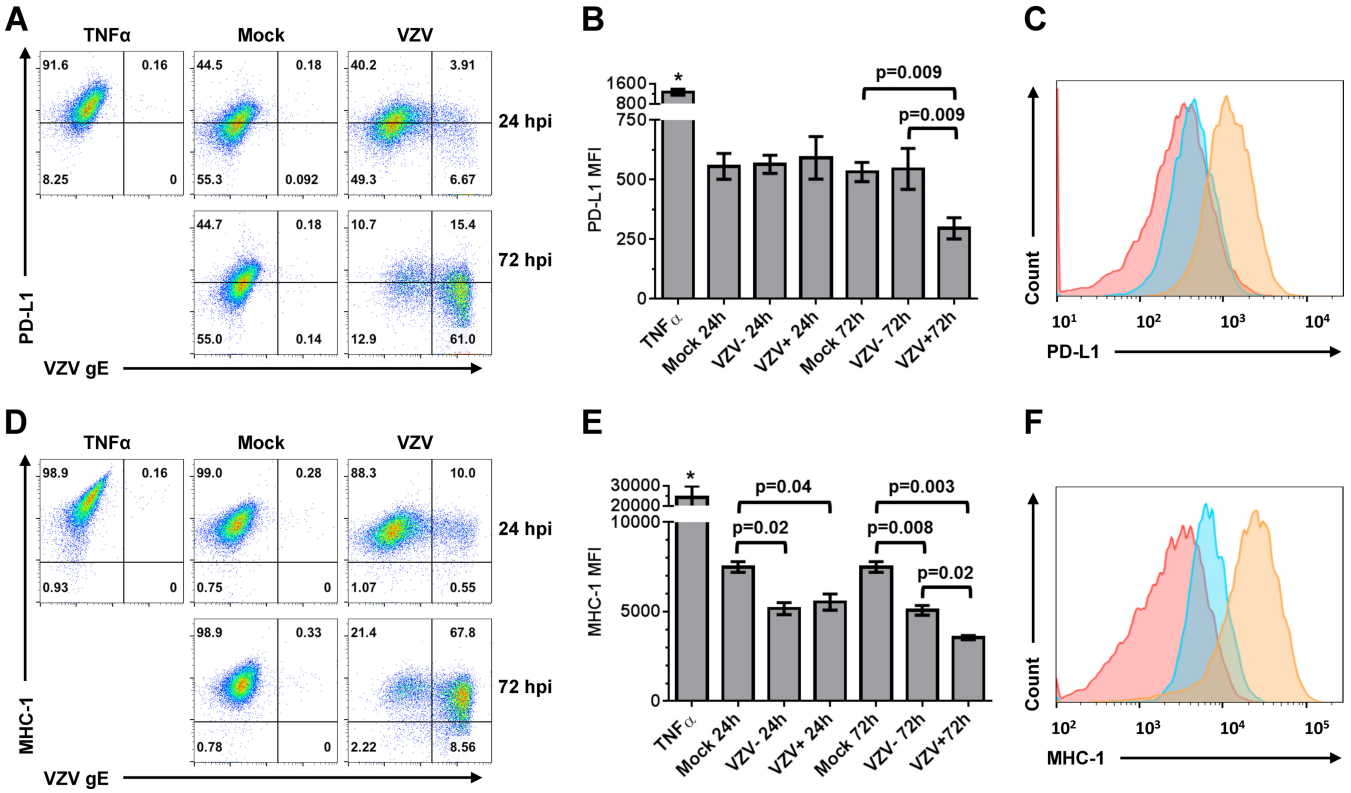

FIG 2 VZV-mediated downregulation of PD-L1 and MHC-I expression in primary human brain vascular adventitial fibroblasts (HBVAFs). Mock- or VZV-infected HBVAFs at 24 and 72 hpi, as well as positive-control TNF-α-treated HBVAFs at 24 h posttreatment, were harvested and analyzed by three-color flow cytometry using anti-VZV gE and anti-PD-L1 antibodies (A to C) or anti-VZV gE and anti-MHC-I antibodies (D to F); cells were gated using isotype and fluorescence-minus-one (FMO) controls. Flow cytometry plots (A) and corresponding bar graphs (B) after immunostaining with VZV gE and PD-L1 antibodies showed a significant reduction in PD-L1 MFI at 72 hpi in VZV-infected (VZV+ 72 h) HBVAFs compared to adjacent uninfected cells (VZV− 72 h; $P = 0.009$) and to mock-infected cells (mock 72 h; $P = 0.009$). (C) Histogram flow cytometry analyses at 72 hpi show total downregulation of PD-L1 MFI expression in VZV^+ (red) cells compared to mock-infected (blue) or TNF-α-treated (orange) cells. Flow cytometry plots (D) and corresponding bar graphs (E) after immunostaining with VZV gE and MHC-I antibodies showed a significant reduction in MHC-I MFI in both VZV-infected HBVAFS at 24 hpi (VZV+ 24 h; $P = 0.04$) and adjacent uninfected cells (VZV− 24 h; $P = 0.02$) compared to mock-infected cells. Similarly, at 72 hpi, there was a significant reduction in MHC-I MFI in both VZV-infected HBVAFS (VZV+ 72 h; $P = 0.003$) and adjacent uninfected cells (VZV− 72 h; $P = 0.008$) compared to mock-infected cells. There was also a significant reduction in MHC-I MFI in VZV-infected HBVAFs compared to adjacent uninfected cells (VZV− 72 h; $P = 0.02$). (F) Histogram flow cytometry analyses at 72 hpi show total downregulation of MHC-I MFI expression in VZV^+ (red) cells compared to mock-infected (blue) or TNF-α-treated (orange) cells. All results shown are representative of 6 independent experiments, with bar graphs representing average MFI values and error bars representing standard deviations. Statistical significance was determined using the Student *t* test. *, $P < 0.001$ for HBVAFs treated with TNF-α for 24 h compared to mock- and VZV-infected HBVAFs analyzed at 24 and 72 hpi.

provided by HFLs and HBVAFs treated with TNF-α and HPNCs treated with IFN-γ for 24 h before analysis (Fig. 5B, column 1). Negative controls were provided by omission of primary antibody (Fig. 5B, column 2).

DISCUSSION

Here, we show that VZV infection of two vascular adventitial cell types, human brain vascular adventitial fibroblasts (HBVAFs) and perineural cells (HPNCs), as well as human fetal lung fibroblasts (HFLs), downregulates expression of PD-L1 and MHC-I within 72 hpi. Several remarkable features emerged from this study.

First, downregulation of PD-L1 in VZV-infected cells is novel in light of prior reports that virus infection upregulates PD-L1 in both immune and nonimmune cells. Specifically, PD-L1 is increased in HIV-infected $CD4^+$ T cells (12) and monocytes (17), Epstein-Barr virus (EBV)-infected Hodgkin lymphoma cells, EBV-transformed lymphoblastoid cell lines (18), and EBV-infected nasopharyngeal carcinoma cell lines (19). Influenza and respiratory syncytial virus induce PD-L1 expression in human lung and pulmonary macrophages in an *ex vivo* model (20). Finally, PD-L1 is induced in adenovirus-infected hepatocytes and hepatitis B virus-infected hepatic carcinoma cells (21). In those instances, virus-induced upregulation of PD-L1 led to increased binding to the PD-1 receptor on immune cells, ultimately resulting in the apoptosis of immune cells and virus persistence.

No prior investigations into the role of VZV-mediated regulation of PD-L1 expression have been reported. However, studies involving herpes simplex virus type 1 (HSV-1), another member of the *Alphaherpesvirinae* subfamily, report conflicting results with regard to PD-L1 expression and viral spread in various cell types. For example, during footpad HSV-1 infection in mice, monoclonal antibody blockade of PD-L1 enhances primary and secondary CD8 T cell immune responses (22). During HSV-1 infection of murine corneas, one study demonstrated that monoclonal antibody blockade of PD-L1 reduced HSV-1-specific CD8 T cells, as well as reduced numbers of CD80-expressing dendritic

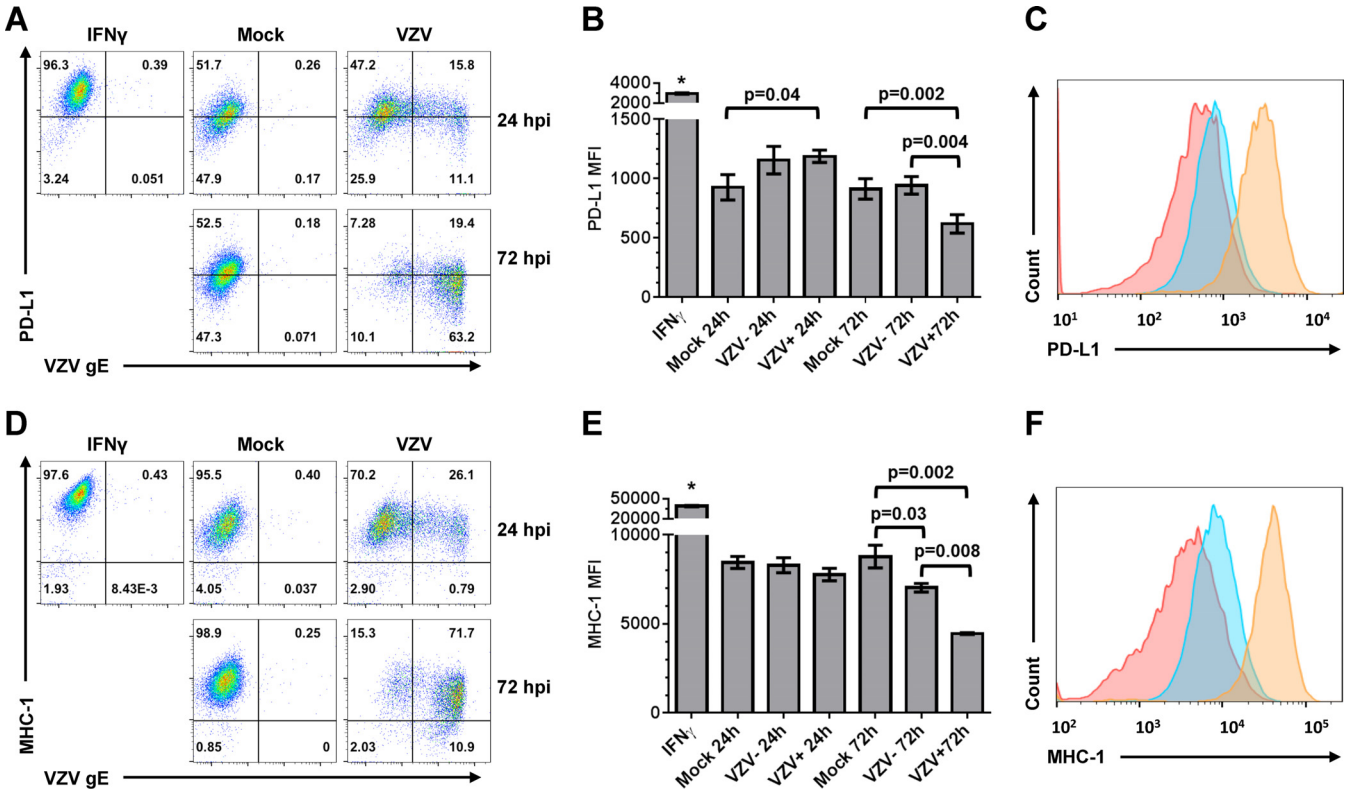

FIG 3 VZV-mediated downregulation of PD-L1 and MHC-I expression in primary human perineural cells (HPNCs). Mock- or VZV-infected HPNCs at 24 and 72 hpi, as well as positive-control IFN-γ-treated HPNCs at 24 h posttreatment, were harvested and analyzed by three-color flow cytometry using anti-VZV gE and anti-PD-L1 antibodies (A to C) or anti-VZV gE and anti-MHC-I antibodies (D to F); cells were gated using isotype and fluorescence-minus-one (FMO) controls. Flow cytometry plots (A) and corresponding bar graphs (B) after immunostaining with VZV gE and PD-L1 antibodies showed a significant induction of PD-L1 MFI in VZV-infected HPNCs at 24 hpi (VZV+ 24 h; $P = 0.04$) compared to mock-infected cells (mock 24 h). At 72 hpi, VZV-infected (VZV+ 72 h) HPNCs had a significant reduction in PD-L1 MFI compared to adjacent uninfected cells (VZV− 72 h; $P = 0.004$) and to mock-infected cells (mock 72 h; $P = 0.002$). (C) Histogram flow cytometry analyses at 72 hpi show total downregulation of PD-L1 MFI expression in VZV^+ (red) cells compared to mock-infected (blue) or IFN-γ-treated (orange) cells. Flow cytometry plots (D) and corresponding bar graphs (E) after immunostaining with VZV gE and MHC-I antibodies showed a significant reduction in MHC-I MFI in VZV-infected HPNCs at 72 hpi (VZV+ 72 h; $P = 0.002$) and adjacent uninfected cells (VZV− 72 h; $P = 0.03$) compared to mock-infected cells. There was also a significant reduction in MHC-I MFI in VZV-infected HPNCs compared to adjacent uninfected cells ($P = 0.008$). (F) Histogram flow cytometry analyses at 72 hpi show total downregulation of MHC-I MFI expression in VZV^+ (red) cells compared to mock-infected (blue) or IFN-γ-treated (orange) cells. All results shown are representative of 6 independent experiments, with bar graphs representing average MFI values and error bars representing standard deviations. Statistical significance was determined using the Student *t* test. *, $P < 0.001$ for HPNCs treated with IFN-γ compared to mock- and VZV-infected HPNCs analyzed at 24 and 72 hpi.

cells and $PD\text{-}L1^+$ dendritic cells, in conjunction with increased viral load (23); in another study, monoclonal antibody blockade of PD-L1 resulted in decreased apoptosis and increased proliferation and IFN-γ secretion by HSV-1-specific CD4 T cells, which exasperated herpetic stromal keratitis (24).

Here, we found that PD-L1 was downregulated in the VZV-infected vascular and lung cells, raising the possibility that apoptosis is not induced in infiltrating immune cells expressing PD-1. In addition, VZV-mediated downregulation of MHC-I occurred prior to PD-L1 downregulation, potentially preventing presentation of viral antigens to these infiltrating immune cells. Taken together, the virus-induced dysregulation of PD-L1 and MHC-I may contribute to the ineffective viral clearance and persistent inflammation which has been observed in virus-infected arteries of patients with VZV vasculopathy. Examination of cerebral arteries from patients as late as 10 months after the onset of VZV vasculopathy revealed viral antigen and persistent inflammation comprised predominantly of $CD4^+$ T cells and macrophages (10); furthermore, adventitial inflammation was associated with an overlying thickened intima, supporting the notion that inflammatory cells secrete soluble factors that contribute to pathological vascular remodeling (25, 26). Interestingly, a similar downregulation of the PD-1/PD-L1 pathway is seen in diseases characterized by persistent inflammation, such as mouse models of lupus-like glomerulonephritis/arthritis, cardiomyopathy, type I diabetes, and autoimmune nephritis (27–30). In multiple sclerosis, polymorphisms that reduce PD-1 activity are associated with progressive disease (31). In experimental allergic encephalitis, genetic or pharmacological blockade of PD-1 or PD-L1 enhances activation and expansion of T cells and worsens central nervous system pathology (32, 33). Finally, in PD-1 knockout mice, brain infarcts are larger and immune infiltrates and microglial activation are greater (34). These findings in various autoimmune diseases have prompted therapeutic targeting to activate the PD-1 pathway and alleviate persistent inflammation and associated symptoms. Programmed death ligand-2 (PD-L2) is the other ligand for PD-1 which inhibits immune cell function similarly to PD-L1; however, PD-L2 is mainly expressed on antigen-presenting cells (11) and

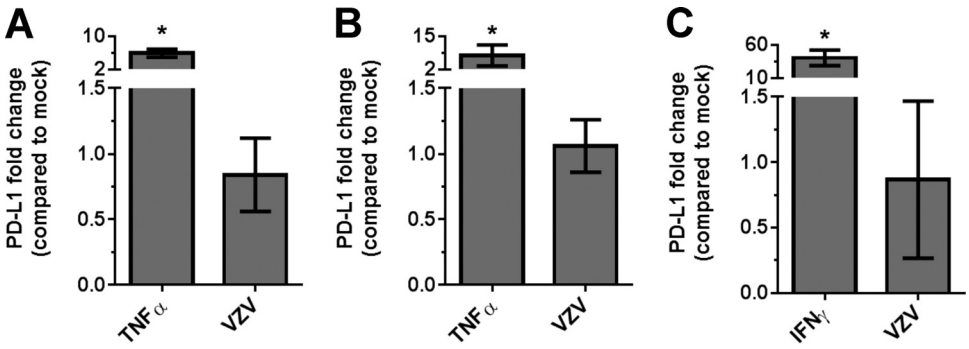

FIG 4 VZV-mediated regulation of *PD-L1* gene expression in mock- and VZV-infected human fetal lung fibroblasts (HFLs), brain vascular adventitial fibroblasts (HBVAFs), and perineural cells (HPNCs). RNA was harvested at 72 hpi from mock- and VZV-infected HFLs, HBVAFs, and HPNCs and then analyzed by quantitative RT-PCR for *PD-L1* mRNA with results normalized to RPL-13a followed by $\Delta\Delta C_T$ analysis. As a positive control for *PD-L1* gene expression, HFLs and HBVAFs were treated with TNF-α and HPNCs were treated with IFN-γ, and then they were harvested for RNA analysis 24 h after treatment. (A) Compared to levels in mock-infected cells, VZV-infected HFL *PD-L1* transcripts were decreased 0.84- ± 0.28-fold, and TNF-α-treated HFL *PD-L1* transcripts were increased 5.96- ± 0.98-fold. (B) Compared to mock-infected cells, VZV-infected HBVAF *PD-L1* transcripts were increased 1.06- ± 0.21-fold, and TNF-α-treated HBVAF *PD-L1* transcripts were increased 7.56- ± 4.12-fold. (C) Compared to mock-infected cells, VZV-infected HPNCs *PD-L1* transcripts were decreased 0.87- ± 0.63-fold, and IFN-γ-treated HPNC *PD-L1* transcripts were increased 40.59- ± 11.64-fold. Bar graphs represent the average *PD-L1* fold change with error bars representing standard deviations from triplicate experiments. Statistical significance was determined using the Student *t* test. *, $P < 0.01$.

was minimally expressed in the cell lines analyzed here (data not shown); therefore, we did not investigate its expression levels during VZV infection.

Second, PD-L1 transcript levels were unchanged in VZV-infected cells, whereas protein was decreased, indicating that regulation occurs posttranscriptionally. The exact mechanism(s) is unclear; however, VZV may induce proteasomal degradation of PD-L1 protein, a notion supported by a previous study showing that VZV induces proteasomal degradation of MHC-I protein via ORF66-dependent phosphorylation that leads to retention of MHC-I in the Golgi apparatus and subsequent degradation (35). VZV-mediated downregulation of other host proteins, such as glial acidic fibrillary protein (GFAP) in astrocytes (36), have been reported and appear to be targeted specifically by viral infection,

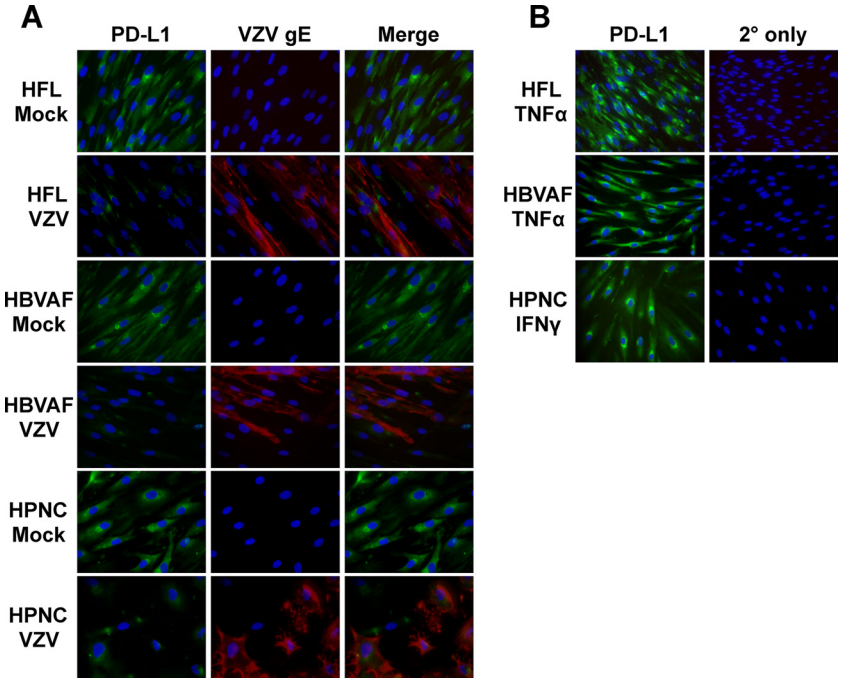

FIG 5 Immunofluorescence analysis of PD-L1 and VZV gE expression in mock- and VZV-infected human fetal lung fibroblasts (HFLs), brain vascular adventitial fibroblasts (HBVAFs), and perineural cells (HPNCs). At 72 hpi, mock- and VZV-infected HFLs, HBVAFs, and HPNCs were analyzed by dual immunofluorescence using a rabbit anti-PD-L1 antibody and a mouse anti-VZV gE antibody. (A) Mock-infected HFLs, HBVAFs, and HPNCs expressed PD-L1 (green) but not VZV gE (red) (rows 1, 3, 5, and 7, respectively), whereas VZV-infected HFLs, HBVAFs, and HPNCs expressed VZV gE with minimal to no expression of PD-L1 (rows 2, 4, 6, and 8, respectively). Magnification, ×600. (B) Positive controls for PD-L1 expression (green) were provided by HFLs and HBVAFs treated with TNF-α, as well as HPNCs treated with IFN-γ for 24 h before analysis (column 1). Negative controls were provided by omission of primary antibody (column 2). Blue color represents DAPI cell nucleus stain. Magnification, ×400.

not complete shutdown of host protein synthesis. Initial reports of VZV-mediated downregulation of MHC-I also showed that transferrin receptor expression was unchanged, indicating that VZV does not downregulate all host proteins during infection (37). Similarly, we did not observe any changes in transferrin receptor expression levels at 72 hpi in any of the cell lines analyzed (data not shown), further supporting VZV-specific MHC-I and PD-L1 downregulation.

Finally, while downregulation of MHC-I in VZV-infected cells is consistent with prior studies (35), concurrent downregulation of MHC-I in uninfected bystander cells at 72 hpi has not been reported. This finding suggests that VZV-infected cells secrete a soluble factor, such as a cytokine, to effect downregulation of MHC-I in adjacent, uninfected bystander cells. Indeed, previous studies have shown that transforming growth factor beta (TGF-β) may suppress MHC expression, since TGF-β-knockout mice have elevated MHC-I and MHC-II (38), while interleukin-10 downregulates MHC-II expression in monocytes to prevent antigen presentation (39). Overall, downregulation of MHC-I would prevent presentation of VZV antigen to CD8 T cells that would lead to clearance of infected cells.

Together, our studies provide a potential mechanism by which persistent inflammation in the absence of effective viral clearance occurs in VZV vasculopathy and VZV infection of the lung. Specifically, VZV-mediated downregulation of PD-L1 in vascular cells may contribute to the persistence of immune cells in VZV vasculopathy, which secrete soluble factors that produce loss of smooth muscle cells, a thickened intima, and stroke (9, 10). Similarly, in VZV-infected lung during primary infection, T cells have yet to encounter viral antigen, and the initial downregulation of MHC-I may prevent clonal expansion of T cells specific for VZV. As infection persists in the lung, PD-L1 downregulation would prevent apoptosis induction in T cells via the PD-1 pathway, and VZV-infected lung cells would be primed to transmit virus to T cells to fulfill their role as the hematogenous carriers of virus to skin during varicella. Further characterization of potential differences in VZV modulation of PD-L1 expression in T cells and neurons is warranted since VZV has a tropism for T cells and establishes latency in neurons.

ACKNOWLEDGMENTS

We thank Marina Hoffman for editorial review and Cathy Allen for manuscript preparation.

This work was supported by Public Health Service grants NS094758 (M.A.N.) and AG032958 (D.G. and M.A.N.) from the National Institutes of Health.

FUNDING INFORMATION

This work, including the efforts of Maria A. Nagel, was funded by HHS | National Institutes of Health (NIH) (NS094758). This work, including the efforts of Donald Gilden and Maria A. Nagel, was funded by HHS | National Institutes of Health (NIH) (AG032958).

This work was supported by Public Health Service grants NS094758 (M.A.N.) and AG032958 (D.G. and M.A.N.) from the National Institutes of Health.

REFERENCES

1. **Gilden DH, Vafai A, Shtram Y, Becker Y, Devlin M, Wellish M.** 1983. Varicella-zoster virus DNA in human sensory ganglia. Nature **306:**478–480. http://dx.doi.org/10.1038/306478a0.
2. **Mahalingam R, Wellish MC, Dueland AN, Cohrs RJ, Gilden DH.** 1992. Localization of herpes simplex virus and varicella zoster virus DNA in human ganglia. Ann Neurol **31:**444–448. http://dx.doi.org/10.1002/ana.410310417.
3. **Kennedy PG, Grinfeld E, Gow JW.** 1998. Latent varicella-zoster virus is located predominantly in neurons in human trigeminal ganglia. Proc Natl Acad Sci U S A **95:**4658–4662. http://dx.doi.org/10.1073/pnas.95.8.4658.
4. **Kennedy PG, Grinfeld E, Gow JW.** 1999. Latent varicella-zoster virus in human dorsal root ganglia. Virology **258:**451–454. http://dx.doi.org/10.1006/viro.1999.9745.
5. **Gilden DH, Gesser R, Smith J, Wellish M, Laguardia JJ, Cohrs RJ, Mahalingam R.** 2001. Presence of VZV and HSV-1 DNA in human nodose and celiac ganglia. Virus Genes **23:**145–147. http://dx.doi.org/10.1023/A:1011883919058.
6. **Nagel MA, Rempel A, Huntington J, Kim F, Choe A, Gilden D.** 2014. Frequency and abundance of alphaherpesvirus DNA in human thoracic sympathetic ganglia. J Virol **88:**8189–8192. http://dx.doi.org/10.1128/JVI.01070-14.
7. **Gilden D, White T, Khmeleva N, Heintzman A, Choe A, Boyer PJ, Grose C, Carpenter JE, Rempel A, Bos N, Kandasamy B, Lear-Kaul K, Holmes DB, Bennett JL, Cohrs RJ, Mahalingam R, Mandava N, Eberhart CG, Bockelman B, Poppiti RJ, Tamhankar MA, Fogt F, Amato M, Wood E, Durairaj V, Rasmussen S, Petursdottir V, Pollak L, Mendlovic S, Chatelain D, Keyvani K, Brueck W, Nagel MA.** 2015. Prevalence and distribution of VZV in temporal arteries of patients with giant cell arteritis. Neurology **84:**1948–1955. http://dx.doi.org/10.1212/WNL.0000000000001409.
8. **Gilden D, White T, Boyer PJ, Galetta KM, Hedley-Whyte ET, Frank M, Holmes D, Nagel MA.** 2016. Varicella zoster virus infection in granulomatous arteritis of the aorta. J Infect Dis **213:**1866–1871. http://dx.doi.org/10.1093/infdis/jiw101.
9. **Nagel MA, Traktinskiy I, Azarkh Y, Kleinschmidt-DeMasters B, Hedley-Whyte T, Russman A, Van Egmond EM, Stenmark K, Frid M, Mahalingam R, Wellish M, Choe A, Cordery-Cotter R, Cohrs RJ, Gilden D.** 2011. Varicella zoster virus vasculopathy: analysis of virus-infected arteries. Neurology **77:**364–370. http://dx.doi.org/10.1212/WNL.0b013e3182267bfa.
10. **Nagel MA, Traktinskiy I, Stenmark KR, Frid MG, Choe A, Gilden D.** 2013. Varicella-zoster virus vasculopathy: immune characteristics of virus-infected arteries. Neurology **80:**62–68. http://dx.doi.org/10.1212/WNL.0b013e31827b1ab9.
11. **Pardoll DM.** 2012. The blockade of immune checkpoints in cancer immunotherapy. Nat Rev Cancer **12:**252–264. http://dx.doi.org/10.1038/nrc3239.
12. **Akhmetzyanova I, Drabczyk M, Neff CP, Neff CP, Gibbert K, Dietze KK, Werner T, Liu J, Chen L, Lang KS, Palmer BE, Dittmer U, Zelinskyy G.** 2015. PD-L1 expression on retrovirus-infected cells mediates immune escape from CD8+ T cell killing. PLoS Pathog **11:**e1005224. http://dx.doi.org/10.1371/journal.ppat.1005224.
13. **Dai S, Jia R, Zhang X, Fang Q, Huang L.** 2014. The PD-1/PD-Ls pathway and autoimmune diseases. Cell Immunol **290:**72–79. http://dx.doi.org/10.1016/j.cellimm.2014.05.006.
14. **Zhang B, Shan H, Li D, Li ZR, Zhu KS, Jiang ZB, Huang MS.** 2012. Different methods of detaching adherent cells significantly affect the detection of TRAIL receptors. Tumori **98:**800–803.
15. **Germanidis G, Argentou N, Hytiroglou P, Vassiliadis T, Patsiaoura K, Germenis AE, Spelestas M.** 2013. Liver FOXP3 and PD1/PDL1 expression is down-regulated in chronic HBV hepatitis on maintained remission related to the degree of inflammation. Front Immunol **4:**207.
16. **Küçük C, Iqbal J, Hu X, Gaulard P, De Leval L, Srivastava G, Au WY, McKeithan TW, Chan WC.** 2011. PRDM1 is a tumor suppressor gene in natural killer cell malignancies. Proc Natl Acad Sci U S A **108:**20119–20124. http://dx.doi.org/10.1073/pnas.1115128108.
17. **Boasso A, Hardy AW, Landay AL, Martinson JL, Anderson SA, Dolan MJ, Clerici M, Shearer GM.** 2008. PDL-1 upregulation on monocytes and T cells by HIV via type I interferon: restricted expression of type I interferon receptor by CCR5-expressing leukocytes. Clin Immunol **129:**132–144. http://dx.doi.org/10.1016/j.clim.2008.05.009.
18. **Green MR, Rodig S, Juszczynski P, Ouyang J, Sinha P, O'Donnell E, Neuberg D, Shipp MA.** 2012. Constitutive AP-1 activity and EBV infection induce PD-L1 in Hodgkin lymphomas and posttransplant lymphoproliferative disorders: implications for targeted therapy. Clin Cancer Res **18:**1611–1618. http://dx.doi.org/10.1158/1078-0432.CCR-11-1942.
19. **Fang W, Zhang J, Hong S, Zhan J, Chen N, Qin T, Tang Y, Zhang Y,**

Kang S, Zhou T, Wu X, Liang W, Hu Z, Ma Y, Zhao Y, Tian Y, Yang Y, Xue C, Yan Y, Hou X, Huang P, Huang Y, Zhao H, Zhang L. 2014. EBV-driven LMP1 and IFN-gamma up-regulate PD-L1 in nasopharyngeal carcinoma: implications for oncotargeted therapy. Oncotarget **5:**12189–12202. http://dx.doi.org/10.18632/oncotarget.2608.

20. **Staples KJ, Nicholas B, McKendry RT, Spalluto CM, Wallington JC, Bragg CW, Robinson EC, Martin K, Djukanovic R, Wilkinson TM.** 2015. Viral infection of human lung macrophages increases PDL1 expression via IFNbeta. PLoS One **10:**e0121527. http://dx.doi.org/10.1371/journal.pone.0121527.
21. **Mühlbauer M, Fleck M, Schütz C, Weiss T, Froh M, Blank C, Schölmerich J, Hellerbrand C.** 2006. PD-L1 is induced in hepatocytes by viral infection and by interferon-alpha and -gamma and mediates T cell apoptosis. J Hepatol **45:**520–528. http://dx.doi.org/10.1016/j.jhep.2006.05.007.
22. **Channappanavar R, Twardy BS, Suvas S.** 2012. Blocking of PDL-1 interaction enhances primary and secondary CD8 T cell response to herpes simplex virus-1 infection. PLoS One **7:**e39757. http://dx.doi.org/10.1371/journal.pone.0039757.
23. **Bryant-Hudson KM, Carr DJ.** 2012. PD-L1-expressing dendritic cells contribute to viral resistance during acute HSV-1 infection. Clin Dev Immunol **2012:**924619.
24. **Jun H, Seo SK, Jeong HY, Seo HM, Zhu G, Chen L, Choi IH.** 2005. B7-H1 (CD274) inhibits the development of herpetic stromal keratitis (HSK). FEBS Lett **579:**6259–6264. http://dx.doi.org/10.1016/j.febslet.2005.09.098.
25. **Stenmark KR, Nozik-Grayck E, Gerasimovskaya E, Anwar A, Li M, Riddle Z, Frid M.** 2011. The adventitia: essential role in pulmonary vascular remodeling. Compr Physiol **1:**141–161.
26. **Stenmark KR, Yeager ME, El Kasmi KC, Nozik-Grayck E, Gerasimovskaya EV, Li M, Riddle S, Frid MG.** 2013. The adventitia: essential regulator of vascular wall structure and function. Annu Rev Physiol **75:**23–47. http://dx.doi.org/10.1146/annurev-physiol-030212-183802.
27. **Nishimura H, Nose M, Hiai H, Minato N, Honjo T.** 1999. Development of lupus-like autoimmune diseases by disruption of the PD-1 gene encoding an ITIM motif-carrying immunoreceptor. Immunity **11:**141–151. http://dx.doi.org/10.1016/S1074-7613(00)80089-8.
28. **Nishimura H, Okazaki T, Tanaka Y, Nakatani K, Hara M, Matsumori A, Sasayama S, Mizoguchi A, Hiai H, Minato N, Honjo T.** 2001. Autoimmune dilated cardiomyopathy in PD-1 receptor-deficient mice. Science **291:**319–322. http://dx.doi.org/10.1126/science.291.5502.319.
29. **Fife BT, Pauken KE, Eagar TN, Obu T, Wu J, Tang Q, Azuma M, Krummel ME, Bluestone JA.** 2009. Interactions between PD-1 and PD-L1 promote tolerance by blocking the TCR-induced stop signal. Nat Immunol **10:**1185–1192. http://dx.doi.org/10.1038/ni.1790.
30. **Reynoso ED, Elpek KG, Francisco L, Bronson R, Bellemare-Pelletier A, Sharpe AH, Freeman GJ, Turley SJ.** 2009. Intestinal tolerance is converted to autoimmune enteritis upon PD-1 ligand blockade. J Immunol **182:**2102–2112. http://dx.doi.org/10.4049/jimmunol.0802769.
31. **Kroner A, Mehling M, Hemmer B, Rieckmann P, Toyka KV, Mäurer M, Wiendl H.** 2005. A PD-1 polymorphism is associated with disease progression in multiple sclerosis. Ann Neurol **58:**50–57. http://dx.doi.org/10.1002/ana.20514.
32. **Latchman Y, Wood CR, Chernova T, Chaudhary D, Borde M, Chernova I, Iwai Y, Long AJ, Brown JA, Nunes R, Greenfield EA, Bourque K, Boussiotis VA, Carter LL, Carreno BM, Malenkovich N, Nishimura H, Okazaki T, Honjo T, Sharpe AH, Freeman GJ.** 2001. PD-L2 is a second ligand for PD-1 and inhibits T cell activation. Nat Immunol **2:**261–268. http://dx.doi.org/10.1038/85330.
33. **Salama AD, Chitnis T, Imitola J, Ansari MJ, Akiba H, Tushima F, Azuma M, Yagita H, Sayegh MH, Khoury SJ.** 2003. Critical role of the programmed death-1 (PD-1) pathway in regulation of experimental autoimmune encephalomyelitis. J Exp Med **198:**71–78. http://dx.doi.org/10.1084/jem.20022119.
34. **Ren X, Akiyoshi K, Vandenbark AA, Hurn PD, Offner H.** 2011. Programmed death-1 pathway limits central nervous system inflammation and neurologic deficits in murine experimental stroke. Stroke **42:**2578–2583. http://dx.doi.org/10.1161/STROKEAHA.111.613182.
35. **Abendroth A, Lin I, Slobedman B, Ploegh H, Arvin AM.** 2001. Varicella-zoster virus retains major histocompatibility complex class I proteins in the Golgi compartment of infected cells. J Virol **75:**4878–4888. http://dx.doi.org/10.1128/JVI.75.10.4878-4888.2001.
36. **Kennedy PGE, Major EO, Williams RK, Straus SE.** 1994. Down-regulation of glial fibrillary acidic protein expression during acute lytic varicella-zoster virus infection of cultured human astrocytes. Virology **205:**558–562. http://dx.doi.org/10.1006/viro.1994.1679.
37. **Cohen JI.** 1998. Infection of cells with varicella-zoster virus down-regulates surface expression in class I major histocompatibility complex antigens. J Infect Dis **177:**1390–1393. http://dx.doi.org/10.1086/517821.
38. **Letterio JJ, Roberts AB.** 1998. Regulation of immune responses by TGF-beta. Annu Rev Immunol **16:**137–161. http://dx.doi.org/10.1146/annurev.immunol.16.1.137.
39. **de Waal Malefyt R, Abrams J, Bennett B, Figdor CG, de Vries JE.** 1991. Interleukin 10 (IL-10) inhibits cytokine synthesis by human monocytes: an autoregulatory role of IL-10 produced by monocytes. J Exp Med **174:**1209–1220. http://dx.doi.org/10.1084/jem.174.5.1209.